Available online at www.sciencedirect.com
SCIENCE DIRECT®
Journal of Sound and Vibration 274 (2004) 445–454
JOURNAL OF SOUND AND VIBRATION
www.elsevier.com/locate/jsvi

Letter to the Editor

Analysis and computation of the vibration spectrum of the cartesian flexible manipulator

M.P. Coleman*, L.A. McSweeney

Department of Mathematics and Computer Science, Fairfield University, Fairfield, CT 06824-5195, USA

Received 11 July 2002; accepted 7 September 2003

1. Introduction

In the vibration control of flexible structures such as robot arms, boundary feedback schemes are employed in order to damp the vibrations and dissipate energy and, thus, to achieve stabilization. Knowing the vibration eigenspectrum is crucial to the process.

Refs. [1,2] deal with the control of the boundary value problem for a flexible robot arm which is strongly clamped to a moving mass, and with a payload attached to the other end. A mass—in practice, an actuator—is attached to the base, as well. The base moves along a straight line which is perpendicular to the beam. Although the model treats motion without friction one could include a friction term. This model is important because it is one of the two standard models for single-link robot arms [1]. (The other is the slewing beam, which models a *rotational* joint at the actuator end.) Also, it is a generalization of the roller-supported-free beam. Of the four natural, energy-conserving boundary conditions which arise in the study of beams (clamped, pinned, roller-supported and free), the roller-supported condition has received significantly less treatment than the other three. Further, while the slewing beam is a generalization of the pinned-free beam, (and the cantilever beam with payload is well studied), we have not been able to find in the literature any other generalizations of this roller-supported condition.

While the vibration of the slewing beam has been fairly well studied, a resonant eigenfrequency analysis of this so-called *Cartesian arm* has not been performed, to our knowledge. Therefore, we investigate the vibration spectrum of this model. However, as the authors of Refs. [1,2] did not derive the model, we first provide a derivation.

The outline of the paper is as follows. In Section 2 we present the model, which consists of an Euler–Bernoulli beam, with the motions of the masses at each end, as well as the rotational motion of the payload (but not of the beam itself) taken into account. It is shown that the model treated in Refs. [1,2] is indeed correct, given a somewhat limiting restriction. In Section 3, we give

*Corresponding author. Tel.: +1-203-254-4000; fax: +1-203-254-4163.
E-mail addresses: mcoleman@fair1.fairfield.edu (M.P. Coleman), lmcsweeney@fair1.fairfield.edu (L.A. McSweeney).

0022-460X/$ - see front matter
doi:10.1016/j.jsv.2003.09.036

a brief derivation of the equation for the exact eigenvalues/eigenfunctions, and we discuss various limiting behaviors of the arm, vis-a-vis the classical Euler–Bernoulli beam. As this transcendental equation is highly non-linear and, as a result, not easy to solve using numerical methods—in particular, it is quite sensitive to the choice of initial guess, and the errors are quite large for the larger eigenvalues—we apply, in Section 4, an asymptotic method due to Keller and Rubinow [3] to the problem. Although, of course, still non-linear, the resulting eigenvalue equation is much better behaved than the *exact* equation. As a result, we may use these *wave* results to suggest values for the initial guess in solving the exact equation, and as an obvious comparison for these results.

Finally, we present actual results in Section 5. We compute the eigenspectrum and plot the eigenfunctions for two sets of data found in Refs. [4,5] (although, as this model seems to be somewhat new, the only data we could find was from references treating the slewing beam). In each case there is good agreement between the *exact* and the *wave* results and, asymptotically, between these results and those of the corresponding Euler–Bernoulli beam. We then investigate the behavior of the spectrum and eigenfunctions as the mass at each end varies from zero to "infinity."

2. Derivation of the equations of motion

We consider the Cartesian robot arm illustrated in Fig. 1. It consists of an actuator at the left end, a flexible beam of length L and uniform linear mass density ρ, and a payload at the right end. In addition, the left end is roller-supported, in other words, it is strongly clamped to a roller, which is free to move vertically without friction.

We set the problem in the inertial reference frame x_0–y_0, while the non-inertial frame x–w is such that the left end of the beam is located at the origin, the undeflected beam lies along the x-axis, and the w- and y_0-axis coincide (Fig. 1).

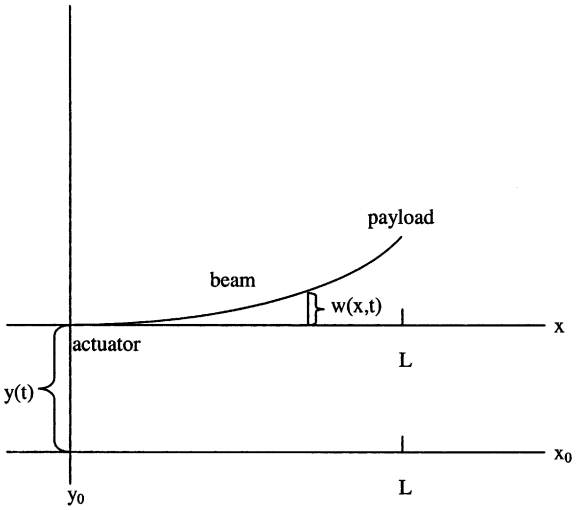

Fig. 1. The Cartesian flexible manipulator.

Except for the behavior of the left and right ends, we assume that the beam is an Euler–Bernoulli (EB) beam. Therefore, the arm moves in a horizontal plane and deflects only transversally. The latter implies that the x- and x_0-co-ordinates of any point along the beam remain identical.

We have, then, $w(x,t)$, the deflection of the beam; $y = y(t)$, the vertical motion of the left end of the beam and $F(t)$, the applied vertical force at the actuator. In addition we have the physical constants m, the mass of actuator; M, the mass of payload; ρ, the linear mass density of the beam; EI, the stiffness of the beam and J, the inertia of the mass at the right end of the beam (with respect to $x_0 = y_0 = 0$).

The EB assumption implies that $w \ll L$. In addition, we shall need to assume that $y \ll L$ below (a fairly restrictive assumption).

We now derive the Lagrangian for the motion of the arm, in terms of the function $z(x,t) = w(x,t) + y(t)$. The kinetic energy at any time t, due to the motion of the left end, is

$$T_1 = \tfrac{1}{2} m\dot{y}(t)^2 = \tfrac{1}{2} m\dot{z}(0,t)^2.$$

That of the beam is

$$T_2 = \tfrac{1}{2}\rho \int_0^L [\dot{w}(x,t) + \dot{y}(t)]^2 \,\mathrm{d}x = \tfrac{1}{2}\rho \int_0^L \dot{z}(x,t)^2 \,\mathrm{d}x,$$

while for the payload we must consider both vertical and rotational motion:

$$T_3 = \tfrac{1}{2} M[\dot{w}(L,t) + \dot{y}(t)]^2 = \tfrac{1}{2} M\dot{z}(L,t)^2$$

and

$$T_4 = \tfrac{1}{2} J\left\{\frac{\mathrm{d}}{\mathrm{d}t}\left[\tan^{-1}\left(\frac{w(L,t)+y(t)}{L}\right)\right]\right\}^2 = \tfrac{1}{2} J\left\{\frac{\mathrm{d}}{\mathrm{d}t}\left[\tan^{-1}\left(\frac{z(L,t)}{L}\right)\right]\right\}^2.$$

Here, *if we assume that* $y(t)$ *is small, then* $z(L,t)$ is small and

$$\tan^{-1}\left[\frac{z(L,t)}{L}\right] \approx \frac{z(L,t)}{L}$$

which, in turn, can be written as

$$\frac{z(L,t)}{L} \approx z_x(L,t).$$

It follows that

$$T_4 = \tfrac{1}{2} J\dot{z}_x(L,t)^2.$$

The potential energy due to the elastic deformation of the beam is the standard expression

$$V = \tfrac{1}{2} EI \int_0^L [w_{xx}(x,t)]^2 \,\mathrm{d}x = \tfrac{1}{2} EI \int_0^L [z_{xx}(x,t)]^2 \,\mathrm{d}x,$$

while the work due to the non-conservative force F is

$$W = F(t)[w(0,t) + y(t)] = F(t)y(t) = F(t)z(0,t).$$

Using Hamilton's principle we derive the equations of motion. Our system of equations consists of the PDE:

$$\rho\ddot{z} + EIz_{xxxx} = 0 \tag{1}$$

with the left-end boundary conditions

$$z_x(0,t) = 0, \tag{2}$$

$$F(t) - EIz_{xxx}(0,t) - m\ddot{z}(0,t) = 0 \tag{3}$$

and the right-end boundary conditions

$$EIz_{xxx}(L,t) - M\ddot{z}(L,t) = 0, \tag{4}$$

$$EIz_{xx}(L,t) + J\ddot{z}_x(L,t) = 0. \tag{5}$$

3. "Exact" solution of the system

As we wish to compute the natural vibration frequencies of system (1)–(5), we set $F(t) \equiv 0$. In Ref. [2], it was proved that the eigenvalues are non-negative real numbers, so we may separate variables by letting

$$z(x,t) = \mathrm{e}^{\mathrm{i}k^2 t}\phi(x),$$

leading to the system

$$a^4k^4\phi(x) - \phi^{(4)}(x) = 0, \tag{6}$$

$$\phi'(0) = 0, \tag{7}$$

$$EI\phi'''(0) - mk^4\phi(0) = 0, \tag{8}$$

$$EI\phi'''(L) + Mk^4\phi(L) = 0, \tag{9}$$

$$EI\phi''(L) - Jk^4\phi'(L) = 0. \tag{10}$$

Here, $a^4 = \rho/(EI)$. The general solution to ODE (6) is

$$\phi(x) = c_1\cos(akx) + c_2\sin(akx) + c_3\cosh(akx) + c_4\sinh(akx). \tag{11}$$

Applying the boundary conditions (7)–(10) leads to a linear system of the form

$$\mathscr{A}[c_1, c_2, c_3, c_4]^{\mathrm{T}} = [0,0,0,0]^{\mathrm{T}}$$

which has a non-trivial solution if and only if

$$\det\mathscr{A} = 0.$$

The characteristic equation is

$$\begin{aligned} &mMJk^5(c\cdot ch-1)+EIa^3(m+M)Jk^4(s\cdot ch+c\cdot sh)\\ &\quad+2E^2I^2a^6Jk^3s\cdot sh+EIamMk^2(s\cdot ch-c\cdot sh)\\ &\quad-2E^2I^2a^4Mkc\cdot ch-E^2I^2a^4mk(c\cdot ch+1)\\ &\quad-a^7E^3I^3(s\cdot ch+c\cdot sh)=0, \end{aligned} \tag{12}$$

where $s=\sin(akL)$, $c=\cos(akL)$, $sh=\sinh(akL)$ and $ch=\cosh(akL)$.

We note that Eq. (12) reduces to what we would expect in the following situations:

$$\begin{aligned} &m=M=J=0: \quad s\cdot ch+c\cdot sh=0 \quad \text{(R–F EB beam)},\\ &m=0; M,J\to\infty: \quad s\cdot ch+c\cdot sh=0 \quad \text{(R–C EB beam)},\\ &m\to\infty; M=J=0: \quad c\cdot ch+1=0 \quad \text{(C–F EB beam)},\\ &m,M,J\to\infty: \quad c\cdot ch-1=0 \quad \text{(C–C EB beam)}. \end{aligned} \tag{13}$$

Here, C stands for "clamped", F for "free" and R for "roller-supported". We investigate this behavior in Section 5.

More interesting is the asymptotic behavior of the spectrum, i.e., as $k\to\infty$:

$$\begin{aligned} &m,M,J\neq 0: \quad \sim c\cdot ch-1=0 \quad \text{(C–C or F–F EB beam)},\\ &m=0; M,J\neq 0: \quad \sim s\cdot ch+c\cdot sh=0 \quad \text{(R–C or R–F EB beam)},\\ &m\neq 0; M=J=0: \quad \sim c\cdot ch+1=0 \quad \text{(C–F EB beam)},\\ &m=M=J=0: \quad \sim s\cdot ch+c\cdot sh=0 \quad \text{(R–C or R–F EB beam)}. \end{aligned} \tag{14}$$

Case 3 in Eq. (14) suggests that, if the mass at an end is non-zero, then that end's asymptotic behavior is the same as if were clamped. This implies that Case 1 corresponds to C–C and Case 2 to R–C.

It is very interesting that we seem to get a sort of bifurcation in the asymptotic spectrum when the mass at an end goes from zero to non-zero. In particular, if $m=0$, the left end is R but if we let $m\neq 0$, no matter how small, the end behaves asymptotically as though it were C. We investigate this behavior, as well, in Section 5 in Fig. 2.

Now, we can use a numerical method on Eq. (12) in order to compute the spectrum for the Cartesian arm. However, the highly non-linear nature of Eq. (12) makes it quite difficult to capture the full spectrum, as the results depend very sensitively on the initial guess.

Instead, we first shall use an asymptotic method to compute the spectrum. Then, we shall use these asymptotic results to inform us as to what we should expect to find for the roots of Eq. (12) and to provide us with initial guesses so that we may find all the roots.

4. Asymptotic estimation of the spectrum

We choose to apply an asymptotic *wave method* of Keller and Rubinow [3,6] to the problem, because it has given accurate results in other beam and plate problems (Refs. [7–11]), and because it is directly constructive (thereby enabling us to compute the eigenfunctions as well). To this end,

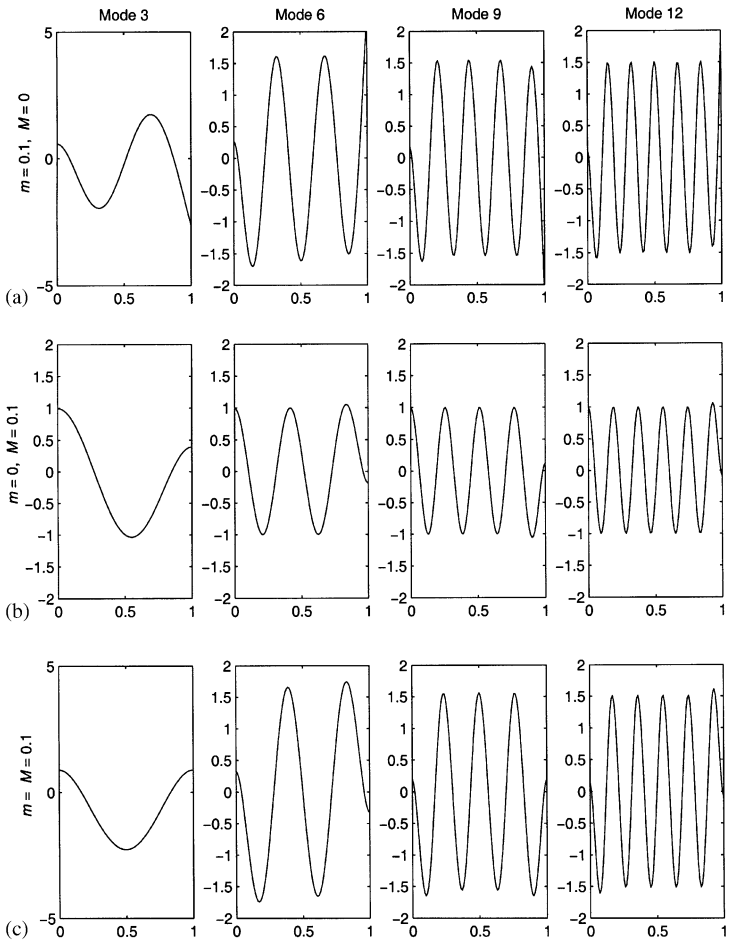

Fig. 2. The eigenfunctions corresponding to the 3rd, 6th, 9th and 12th *exact* frequencies from Example 2 with (a) $m = 0.1$ and $M = 0$, (b) $m = 0$ and $M = 0.1$ and (c) $m = M = 0.1$.

we form the *wave solution*

$$z(x,t) = \mathrm{e}^{-\mathrm{i}k^2 t}[A\mathrm{e}^{-\mathrm{i}kax} + B\mathrm{e}^{\mathrm{i}kax} + C\mathrm{e}^{-\mathrm{a}kx} + D\mathrm{e}^{-ka(L-x)}] \tag{15}$$

of system (1) and apply boundary conditions (2)–(5) to this solution. The conditions given in Eqs. (2) and (3) lead to the *left-end reflection relation*

$$\begin{bmatrix} 1 & 0 \\ 1 & 0 \end{bmatrix} \begin{bmatrix} C \\ D \end{bmatrix} = \underbrace{\begin{bmatrix} -i & i \\ \frac{\mathrm{i}EIa^3 - mk}{EIa^3 + mk} & -\frac{\mathrm{i}EIa^3 + mk}{EIa^3 + mk} \end{bmatrix}}_{R_1} \begin{bmatrix} A \\ B \end{bmatrix}.$$

Similarly the conditions given by Eqs. (4) and (5) give us the *right-end reflection relation*

$$\begin{bmatrix} 0 & 1 \\ 0 & 1 \end{bmatrix} \begin{bmatrix} C \\ D \end{bmatrix} = \underbrace{\begin{bmatrix} \frac{EIa-ik^3J}{EIa-k^3J} & \frac{EIa+ik^3J}{EIa-k^3J} \\ -\frac{iEIa^3+Mk}{EIa^3+Mk} & \frac{iEIa^3-Mk}{EIa^3+Mk} \end{bmatrix}}_{R_2} \begin{bmatrix} e^{-ikaL} & 0 \\ 0 & e^{ikaL} \end{bmatrix} \begin{bmatrix} A \\ B \end{bmatrix}.$$

We note that $\det R_2 \neq 0$ and $\det R_1 = 0 \Leftrightarrow k = 0$. It follows that

$$\underbrace{\left\{ \begin{bmatrix} e^{ikaL} & 0 \\ 0 & e^{-ikaL} \end{bmatrix} R_2^{-1} \begin{bmatrix} 0 & 1 \\ 0 & 1 \end{bmatrix} - R_1^{-1} \begin{bmatrix} 1 & 0 \\ 1 & 0 \end{bmatrix} \right\}}_{R_3} \begin{bmatrix} C \\ D \end{bmatrix} = \begin{bmatrix} 0 \\ 0 \end{bmatrix}. \tag{16}$$

Finally, Eq. (16) has non-trivial solutions if and only $\det R_3 = 0$ which, after *much* simplification, leads to

$$f_1(k)\cos(kaL) - f_2(k)\sin(kaL) = 0, \tag{17}$$

where

$$f_1(k) = E^3I^3a^7 + E^2I^2a^4(2M+m)k + EIamMk^2 - EIa^3(m+M)Jk^4 - mMJk^5$$

and

$$f_2(k) = -E^3I^3a^7 + mEIaMk^2 + 2E^2I^2a^6Jk^3 + EIa^3(m+M)Jk^4.$$

We note that if we let $k \to \infty$ in Eq. (17), the results agree with the asymptotic results found earlier in Eq. (14). We solve Eq. (17) by rewriting it as

$$-kaL + \tan^{-1}\left(\frac{f_1(k)}{f_2(k)}\right) + n\pi = 0, \quad n \in Z. \tag{18}$$

5. Results and comparisons

We begin our computational work by considering two examples which involve data found in the literature. However, as we have not found any data for this Cartesian manipulator, the data we select is from Refs. [4,5], each of which studies the slewing beam. Therefore, some minor adjustments have been necessary. Let us note here that, although we do not list it below, it is easy to show that $k = 0$ always is an eigenvalue, with constant eigenfunction. This represents a rigid body motion, of course.

In each case, we apply the IMSL routine DNEQF [12], which uses the Levenberg–Marquardt algorithm, to the characteristic equation (12) and to the wave method equation (18). For each root k, DNEQF measures the error as $[g(k)]^2$, where $g(k)$ is the left side of the equation being solved. As a rule, we find that the errors involved in solving Eq. (12) usually are very small for the first few (usually two) eigenvalues, after which the error increases rapidly. This is to be expected given that $\exp(akl)$ appears many times in that equation. As for the wave method equation (18),

the errors generally are quite small for *all* of the eigenvalues computed—the one glaring exception that shows up in some cases (as mentioned below) is in the computation of the lowest eigenvalue, a common occurrence when using such asymptotic methods. In these cases, we believe that we are safe in assuming that the "exact" solution is correct, given that the error is quite small. However, we presumably may apply a perturbation method to the wave method results, as in Ref. [11], to obtain better agreement.

We also provide the solutions for the corresponding EB beams as mentioned in Eq. (14). These frequencies were computed using the Legendre-tau spectral method, which entails separating $w(x,t) = e^{\lambda t}\phi(x)$ and expressing ϕ as a truncated series of Legendre polynomials,

$$\phi(x) = \sum_{i=0}^{n} a_n P_n(x).$$

The eigenvalue problem is solved using the IMSL routine DGVRG [12]. In each case, we have used $n = 100$ and, comparing results for $n = 100$ and 102, all results converge to at least four decimal places. These results agree well with those appearing elsewhere in the literature (e.g., in Ref. [13]; however, we have not found any results for beams subject to the roller-supported boundary condition at either end).

Finally, all figures were done using MATLAB.

Our first example (Example 1) considers the data found in Ref. [4]. Here, $E = 2.1 \times 10^{10}$ N/m^2, $I = 1.167 \times 10^{-11}$ m^4, $L = 0.7$ m and $\rho = 2.97$ kg/m. Also, as Ref. [4] takes the mass of the payload to be 0.117 kg, we use this value for the masses m and M. Specifically, Table 1 provides the spectra for the above data and for the following values of the masses: (a) $m = 0.117$, $M = 0$ and (b) $m = 0$, $M = 0.117$. In each case we compute the first 10 eigenvalues k, along with the 20th, 30th, 40th and 50th eigenvalues to show the convergence.

So, in Table 1(a), we compare the exact frequencies in column 1 with the wave frequencies in column 2 and the frequencies for the clamped–free EB beam in column 3. In addition, we provide in parentheses the corresponding errors. We include only "small" errors, and we have arbitrarily chosen to list only errors which are approximately 1 or smaller. (However, it is interesting to note, for example, that in computing the fourth *exact* eigenvalue, one initial guess leads to a value of 15.7256 with an error of about 31, while a different initial guess gives us 15.7258 with an error greater than 150,000. This is a common occurrence with these *exact* computations.) From Table 1(a), along with the inspection of the eigenfunctions, it seems that both methods capture the full spectrum. We have good agreement between the two methods and, asymptotically, between each and the corresponding C–F EB beam. We have similar results in Table 1(b).

For Example 2 we use the data provided by Ref. [5]: $E = 6.9 \times 10^{10}$ N/m^2, $I = 8.31934 \times 10^{-11}$ m^4, $L = 1.0$ m and $\rho = 0.233172$ kg/m. Again, Ref. [5] treats the slewing beam, and treats only the case where the mass of the payload is zero. Here, we provide the *eigenmodes* for the Cartesian beam in Fig. 1 with the above data and with the following values for the masses: (a) $m = 0.1$, $M = 0$, (b) $m = 0$, $M = 0.1$ and (c) $m = M = 0.1$.

Now, we suggested earlier that if a mass is non-zero, then that end should behave, asymptotically, as though it were clamped. Indeed, this statement is borne out by Fig. 2. In particular, if we look at Fig. 2(c), we see that, only after 12 modes, the eigenfunctions are close to that of the C–C EB beam.

Table 1
Comparison of the first 10 frequencies, along with the 20th, 30th, 40th and 50th frequencies, for the Cartesian manipulator with data given by Example 1, and with (a) $m = 0.117$ and $M = 0$ and (b) $m = 0$ and $M = 0.117$

(a) Exact (error)	Wave (error)	C–F
3.16193 (1.2E−10)	3.05374 (2.5E−16)	2.55502
7.31150 (1.2E−4)	7.04942 (5.9E−16)	6.39617
11.5139 (1.0)	11.1085 (8.6E−13)	10.7029
15.7256	15.2511 (1.7E−13)	14.9825
19.9471	19.4489 (6.4E−18)	19.2633
24.1767	23.6782 (2.6E−14)	23.5440
28.4128	27.9257 (2.1E−13)	27.8248
32.6545	32.1838 (4.5E−13)	32.1055
36.9007	36.4487 (6.0E−13)	36.3863
41.1509	40.7179 (6.5E−13)	40.6670
…	…	…
(20th) 83.7753	83.4872 (1.2E−13)	83.4725
(30th) 126.499	126.287 (3.1E−24)	126.565
(40th) 169.259	169.092 (2.8E−23)	169.096
(50th) 212.036	211.899 (2.9E−23)	211.898
(b) Exact (error)	Wave (error)	R–C
2.56648 (2.6E−11)	2.54142 (1.9E−12)	
4.69123(4.7E−7)	4.69095 (2.7E−16)	3.15826
8.46337 (2.1)	8.46336 (2.4E−18)	7.49828
12.6215	12.6215 (4.0E−14)	11.8505
16.8265	16.8275 (3.5E−16)	16.0531
21.0495	21.0495 (2.9E−17)	20.3342
25.2805	25.2806 (6.2E−18)	24.6146
29.5184	29.5182 (2.2E−18)	28.8953
33.7611	33.7610 (8.9E−19)	33.1761
38.0080	38.0080 (4.2E−19)	37.4568
…	…	…
(20th) 80.6110	80.6110 (1.7E−21)	80.2649
(30th) 123.323	123.323 (1.1E−21)	123.074
(40th) 166.076	166.076 (4.2E−20)	165.880
(50th) 208.848	208.848 (1.0E−19)	208.687

Lastly, we would like to investigate the behavior of the Cartesian manipulator as the masses vary from small to large. So for Table 2, we have chosen each of the beam constants to be unity: $E = 1.0\ \mathrm{N/m^2}$, $I = 1.0\ \mathrm{m^4}$, $L = 1.0\ \mathrm{m}$, $\rho = 1.0\ \mathrm{kg/m}$. (We note that these choices are physically realistic, as these values of EI, L and ρ are of the same order as in the previous examples.)

For Table 2, we set $M = 0$ and we list the first eight frequencies for various values of m, from $m = 0$ (R–F) to, presumably, $m = \infty$ (C–F). Indeed, we see that as m increases, the frequencies decrease monotonically from those of the R–F EB beam to those of the C–F EB beam. (We have checked numerous other values of m, and they have not contradicted this statement. The *wave* results agree, as well.)

Table 2
Comparison of the first 8 frequencies for the Cartesian manipulator with data given by Eq. (19), with $M = 0$ and with various increasing values of m

R–F	$m = 0.01$	$m = 0.05$	$m = 0.1$	$m = 0.5$	$m = 1$	$m = 3$	$m = 6$	$m = 10$	$m = 30$	C–F
2.3650	2.3564	2.3250	2.2912	2.1362	2.0540	1.9546	1.9185	1.9022	1.8845	1.8751
5.4978	5.4709	5.3783	5.2887	4.9820	4.8686	4.7618	4.7294	4.7156	4.7014	4.6941
8.6394	8.5982	8.4665	8.3531	8.0509	7.9657	7.8952	7.8754	7.8673	7.8590	7.8548
11.781	11.726	11.560	11.432	11.147	11.078	11.025	11.010	11.005	10.999	10.996
14.923	14.854	14.661	14.524	14.260	14.203	14.160	14.149	14.144	14.140	14.137
18.064	17.982	17.766	17.626	17.382	17.333	17.298	17.277	17.285	17.281	17.278
21.206	21.111	20.875	20.735	20.509	20.467	20.436	20.428	20.425	20.422	20.420
24.347	24.240	23.989	23.849	23.640	23.603	23.576	23.569	23.566	23.563	23.562

References

[1] Z.H. Luo, N. Kitamura, B.Z. Guo, Shear force feedback control of flexible robot arms, *IEEE Transactions on Robotics and Automation* 11 (5) (1995) 760–765.
[2] X. Hou, S. Tsui, A control theory for a Cartesian flexible robot arm, *Journal of Mathematical Analysis and Applications* 225 (1998) 265–288.
[3] J.B. Keller, S.I. Rubinow, Asymptotic solution of eigenvalue problems, *Annals of Physics* 9 (1960) 24–75.
[4] F. Bellazza, L. Lanari, G. Ulivi, Exact modelling of the flexible slewing link, *IEEE Robotics and Automation Conference*, Cincinnati, OH, 1990.
[5] H. Krishnan, Bounded-input Discrete-times Control of a Single-link Flexible Beam, M.Sc.Thesis, Department of Electrical Engineering, University of Waterloo, Ont., Canada, 1988.
[6] G. Chen, J. Zhou, The wave propagation method for the analysis of boundary stabilization in vibrating structures, *SIAM Journal of Applied Mathematics* 50 (1990) 1254–1283.
[7] M.P. Coleman, G. Chen, J. Zhou, Analysis of vibration eigenfrequencies of a thin plate by Keller–Rubinow's wave method: clamped boundary conditions and rectangular geometry, *SIAM Journal of Applied Mathematics* 51 (1991) 967–983.
[8] M.P. Coleman, H.K. Wang, Analysis of the vibration spectrum of a Timoshenko beam with boundary damping by the wave method, *Wave Motion* 17 (1993) 223–239.
[9] M.P. Coleman, Analysis of vibration by the wave propagation method and Bolotin's method for a rectangular thin plate with at least one side roller-supported, *Wave Motion* 25 (2) (1997) 169–180.
[10] M.P. Coleman, G. Chen, Improving low order eigenfrequency estimates derived from the wave propagation method for an Euler–Bernoulli beam, *Journal of Sound and Vibration* 204 (4) (1997) 696–704.
[11] M.P. Coleman, Vibration eigenfrequency analysis of a single-link flexible manipulator, *Journal of Sound and Vibration* 212 (1) (1998) 109–202.
[12] IMSL Math/Library: Fortran Subroutines for Mathematical Applications, IMSL, Houston, TX, 1987.
[13] D. Young, R.P. Felgar Jr., *Tables of Characteristic Functions Representing Normal Modes of Vibration of a Beam*, Engineering Research Series, No. 44, The University of Texas, Austin, TX, 1949.